

A simple strategy to realize biomimetic surfaces with controlled anisotropic wetting

Dong Wu,¹ Qi-Dai Chen,^{1,a)} Jia Yao,¹ Yong-Chao Guan,¹ Jian-Nan Wang,¹ Li-Gang Niu,¹ Hong-Hua Fang,¹ and Hong-Bo Sun^{1,2,a)}

¹State Key Laboratory on Integrated Optoelectronics, College of Electronic Science and Engineering, Jilin University, 2699 Qianjin Street, Changchun 130012, People's Republic of China

²College of Physics, Jilin University, 119 Jiefang Road, Changchun 130023, People's Republic of China

(Received 22 October 2009; accepted 29 December 2009; published online 5 February 2010)

The study of anisotropic wetting has become one of the most important research areas in biomimicry. However, realization of controlled anisotropic surfaces remains challenging. Here we investigated anisotropic wetting on grooves with different linewidth, period, and height fabricated by laser interference lithography and found that the anisotropy strongly depended on the height. The anisotropy significantly increased from 9° to 48° when the height was changed from 100 nm to $1.3 \mu\text{m}$. This was interpreted by a thermodynamic model as a consequence of the increase of free energy barriers versus the height increase. According to the relationship, controlled anisotropic surfaces were rapidly realized by adjusting the grooves' height that was simply accomplished by changing the resin thickness. Finally, the perpendicular contact angle was further enhanced to $131^\circ \pm 2^\circ$ by surface modification, which was very close to $135^\circ \pm 3^\circ$ of a common grass leaf. © 2010 American Institute of Physics. [doi:10.1063/1.3297881]

A wealth of surfaces in nature not only exhibit good hydrophobic ability but also behave directional wetting, such as the rice leaf,¹ the wings of the butterfly,² the trionum flower,³ the duck feather,⁴ and the shark skin.⁵ This phenomenon, crucial for the natural species surviving, is known as *anisotropic wetting*. It is considered that the directional arrangement of microstructures was the key reason for anisotropy. Surfaces with controlled anisotropic wetting restrict liquids flow to desired directions, and are expected to greatly improve the functions of, for example, microfluidic devices^{6,7} and evaporation-driven formation of nanopattern.^{8,9} The potential applications have attracted lasting research efforts.^{1,9-13} For example, Jiang *et al.*¹ grew aligned carbon nanotubes to mimic the surface of a rice leaf; Morita *et al.*¹⁰ reported macroscopic anisotropy on line patterned surfaces of fluoroalkylsilane monolayers by vacuum ultraviolet lithography; Zhao *et al.*¹¹ prepared submicrometer periodic grooved surface on azobenzene polymer films by laser interference. Despite of these exciting works, precisely controlling anisotropic wetting which is highly desired in practical applications⁶⁻⁹ remains challenging because of the lack of a systematic study and deep insight into physics of anisotropic wetting. Until now it is unclear how to control anisotropy and it is also unknown whether it is possible to develop a simple approach to realize controllable anisotropy. In addition, the anisotropy on submicrometer scale periodic grooves has been found weak, only about 10° ,¹¹ as is out of general expectation.

In this letter, we systemically investigated anisotropic wetting behaviors on groove structures with different periods, linewidths, and heights fabricated by interference lithography.¹⁴⁻¹⁶ Importantly, we found that the anisotropic wetting strongly depended on the height, and weakly on the period and linewidth in the common microfabrication scale,

about the magnitude of several micrometers. This agrees well with the theoretical results calculated by a thermodynamic model.^{17,18} With optimal parameters, artificial biomimetic surfaces with controlled anisotropy were realized.

Shown in Figs. 1(a) and 1(c) are bird-view scanning electron microscope (SEM) images of $2 \mu\text{m}$ period and 400 nm height grooves structures with different linewidths. The grooves with several micrometers period were the most common and useful structures for studying anisotropic wetting, here we also focused on this regime. Four kinds of grooves with widths from 600 to 1500 nm were obtained by controlling the laser exposure dosage. The exposure time was

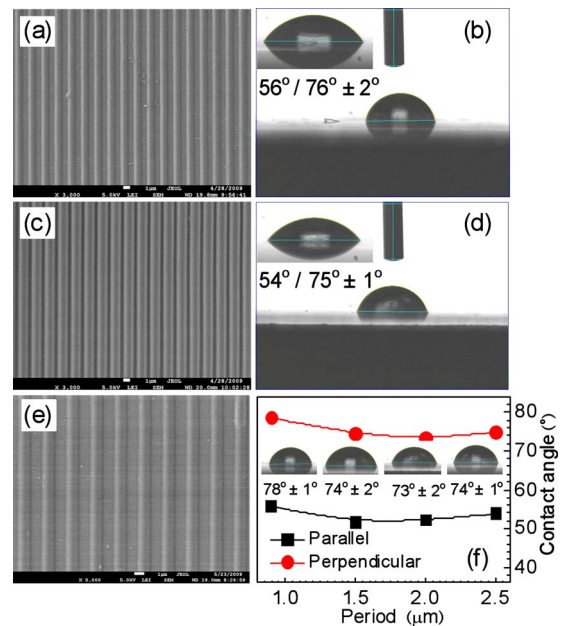


FIG. 1. (Color online) Anisotropic wetting on grooves with different linewidths and periods. (a) and (c) SEM images of $2 \mu\text{m}$ period and 400 nm height grooves structures with different linewidths. (b) and (d) the corresponding CA. (e) $2.5 \mu\text{m}$ period groove. (f) The CA measurement curve.

^{a)}Authors to whom correspondence should be addressed. Electronic addresses: hbsun@jlu.edu.cn and chenqd@jlu.edu.cn.

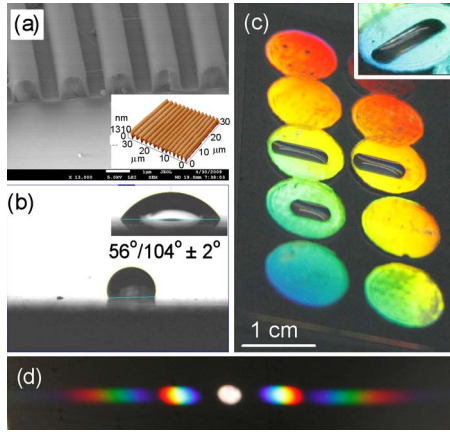


FIG. 2. (Color online) Strongly anisotropic wetting on a 1.3 μm -height groove and its optical properties. (a) 45° tilted-view SEM image of the groove. The inset is the AFM measurement. (b) The corresponding CA. (c) A camera photo of the groove sample with ten grooved regions. (d) An iridescent diffraction pattern of the groove.

changed while the power keeps 50 mW. The durations were 14, 16, 18, and 21 s for groove widths 600 and 900 nm [Fig. 1(a)], 1.2 and 1.5 μm [Fig. 1(c)], respectively. The contact angle (CA) measurement [Figs. 1(b) and 1(d)] was made by a Contact Angle System OCA 20 (DataPhysics Instruments GmbH, Germany). θ_1 and θ_2 were defined as the CA measured in the directions perpendicular and parallel to the longitudinal axis of the grating, and $\Delta\theta = \theta_1 - \theta_2$ was defined as the degree of wetting anisotropy. We could find that the perpendicular CAs were evidently larger than the parallel ones for all grooves because a water droplet tended to flow along the groove. When it spreads along the perpendicular direction, it has to overcome the energy barrier exerted by the grooves. However, it was noted that all the $\Delta\theta$ was around 20° for different grooves and the change for both of θ_1 and θ_2 was not pronounced. Besides the groove linewidth, the influence of period was also studied. The groove period $d = \lambda / (2 \sin \theta)$ is determined by the incident angle θ and the laser wavelength λ . Four kinds of periods 0.9, 1.5, 2, and 2.5 μm [Fig. 1(e)] was obtained under $\theta = 11.4^\circ$, 6.8° , 5.1° , and 4° , respectively. The $\Delta\theta$'s [Fig. 1(f)] for four kinds of periods are between 21° and 23°. There are no obvious differences in anisotropic wetting behaviors. The reason may be that both of the parameters belong to the horizontal direction, and the horizontal variations ($< 2 \mu\text{m}$) of the groove do not significantly cause the increase of FE barriers, which is in accordance with the results reported by Mortia *et al.*¹⁰

Height, which is controlled by the thickness of the resin NOA 61, is the only parameter along the vertical direction of groove. Shown in Fig. 2(a) is 45° tilted-view SEM image of the cross section of 1.3 μm height [the AFM image in the inset of Fig. 2(a)] groove. To our surprise, the θ_1 reached as much as $104^\circ \pm 2^\circ$, while the θ_2 kept $56^\circ \pm 1^\circ$ [Fig. 2(b)]. Due to the strong anisotropy, the droplet along the groove direction became very long, as shown in Fig. 2(c), which was a sample with ten grooved regions ($\sim 600 \text{ mm}^2$). Due to the scattering and diffraction of periodic grooves, the surface shows brilliant iridescence which changes from purple to green [The inset of Fig. 2(c)] under different viewed angles. Furthermore, an iridescent diffraction pattern [Fig. 2(d)] was obtained when the grooves were illuminated under white light, just like the one of the *Hibiscus trionum* flowers.³

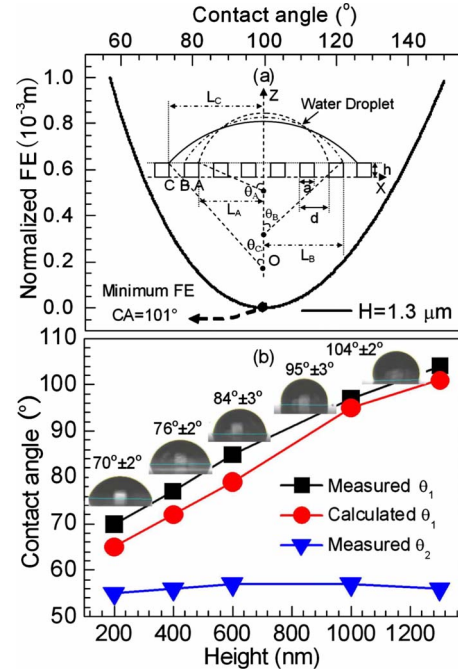


FIG. 3. (Color online) The theoretical calculation of surface FE and the equilibrium CA by a thermodynamic analysis. (a) The surface FE barrier calculation with respect to CA for groove with 1.3 μm height. The inset is the two-dimensional model schematic cross section of groove surface. (b) The strongly dependence between the groove height and anisotropy.

In order to better understand the physical mechanism of anisotropic wetting on the groove, a thermodynamic model¹⁸ was developed to calculate the change in the surface FE as a function of the instantaneous CA during the three-phase contact line moving along the two orthogonal directions. The wetting in our case is in the noncomposite state [the inset in Fig. 3(a)], where the water completely penetrates into the grooves, because the θ_1 strongly depends on the height. The magnitude of the FE barriers increases as the groove height increases, which could lead to the increase in the degree of wetting anisotropy. For the model, provided that the droplet area was constant, an equation was deduced from geometrical analysis to calculate the θ from A to B

$$\theta_A \times L_A^2 / \sin^2 \theta_A - L_A^2 \times \text{ctg} \theta_A = \theta_B \times L_B^2 / \sin^2 \theta_B - L_B^2 \times \text{ctg} \theta_B, \quad (1)$$

where the initial θ_A is chosen as 150° , L_A is 1 mm, $L_B = L_A + a$ and θ_0 is the CA for the flat surface. Then, the relative FE barrier for AB and BC section¹⁸ was calculated and the whole FE barrier curve was obtained.

The FE barrier with respect to CA for groove with 1.3 μm height was calculated, as shown in Fig. 3(a). The F was normalized with respect to the surface tension r^{la} between liquid and gas state and the FE unit will be mm. From the FE barrier curve, we see that there are a minimum FE at 101° , which means the equilibrium state for the water droplet on the grooved surface because the least energy state is steadiest for a system. The experimental value $104^\circ \pm 2^\circ$ agreed well with the theoretical result. With the same calculation method, the FE barrier for the previous 400 nm height groove was obtained. The equilibrium CA was about 72° , which was very close to the measured value $76^\circ \pm 2^\circ$. The small difference $\sim 4^\circ$ was partially caused by the measurement error. In addition, the groove shape we assumed in

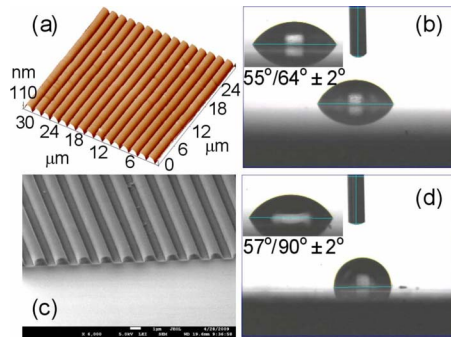


FIG. 4. (Color online) Controlled anisotropic wetting by changing the groove height. (a) The AFM image of a 100 nm height groove. (b) The weak anisotropy $\sim 9^\circ$ because of its smaller height. (c) 45° tilted-view SEM image of the 800 nm height groove. (d) The measured CA was just as what we expected along the deduction from Fig. 3(b).

numerical analysis was square,^{17,18} which had small error compared with the actual cross section of groove. This also affected the difference of anisotropy. To further investigate the relationship between the height and the anisotropy, groove structures with different heights, e.g., 200, 600, and 1000 nm were prepared, and the measured CA's [Fig. 3(b)] were in accordance with the theoretical results. It was evidently seen that the anisotropy strongly depended on the groove height. This made it possible for us to precisely control the degree of the anisotropy by changing the groove height.

To verify this possibility, we freely selected certain angle, for example, 90° . Along the curve in Fig. 3(b), we deduced that the groove height was about 800 nm. Then, by controlling the thickness of the resin, 800 nm height grooves [Fig. 4(c)] was realized and the measured CA was $90^\circ \pm 2^\circ$, just as what we expected. To further verify the possibility of realizing controlled anisotropy, a smaller anisotropy, e.g., 65° would be obtained when the height was around 100 nm according to theoretical analysis. Experimentally, the measured CA on 100 nm-height groove surface [Fig. 4(a)] was about $64^\circ \pm 2^\circ$ [Fig. 4(b)]. The anisotropy was only 9° , which was very close to the results reported by Zhao *et al.*¹¹ They obtained the degree of the anisotropy 9.8° when the height was 127 nm. According to our studies, we deduce that the weak anisotropy on submicrometer grooves¹¹ is mainly caused by the small height (<150 nm). Likewise, the reason for the weak anisotropy wetting on the line-patterned surface of fluoroalkylsilane monolayer (~ 100 nm) reported by Morita *et al.*¹⁰ is also the small height.

For most natural anisotropic surfaces, the CAs along both of the parallel and perpendicular directions are very large ($>120^\circ$) because larger CA is beneficial for water to roll down. For example, the θ_1 and θ_2 are about $135^\circ \pm 3^\circ$ and $120^\circ \pm 2^\circ$ [the insets in Figs. 5(a) and 5(b)] for a common grass leaf. From the SEM images [Figs. 5(a) and 5(b)], we can find that the surface microstructures are in directional arrangement [the white arrow in Fig. 5(a)]. Although the $\Delta\theta$ is only 15° , it is enough for living species to control the water movement direction. For our grooved surface, in order to increase both of the θ_1 and θ_2 , we adopted low-surface-energy fluoroalkylsilane^{19,20} to modify the $1.3 \mu\text{m}$ height groove. After surface modification, the θ_1 was increased from $104^\circ \pm 2^\circ$ [Fig. 2(b)] to $131^\circ \pm 2^\circ$ [Fig. 5(c)] and θ_2 was enhanced from $56^\circ \pm 1^\circ$ [the inset of Fig. 2(b)] to

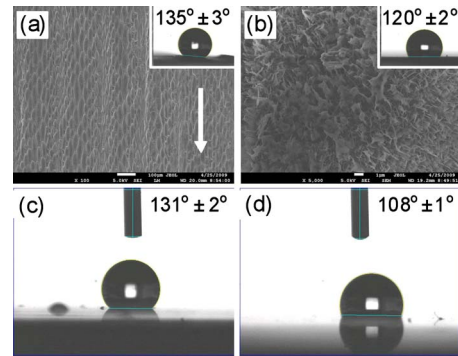


FIG. 5. (Color online) (a) and (b) are SEM image of a common grass leaf surface and its magnified SEM image. The insets are the measured θ_1 and θ_2 . (c) and (d) are the θ_1 and θ_2 enhanced by a fluoroalkylsilane modification on $1.3 \mu\text{m}$ height groove surface.

$108^\circ \pm 1^\circ$ [Fig. 5(d)]. This result was very close to the theoretical θ_1 133° by the FE barrier calculation.

In conclusion, anisotropic wetting behaviors on groove structures with different parameters were systemically studied. Specially, we found the strongly dependence between the anisotropy and the height. Then, we proposed to precisely control anisotropy by adjusting the grooves' height. This method was very simple and easily realized by laser interference lithography. Finally, the CAs were enhanced by surface modification and the wetting property of artificial grooved surfaces was more close to those natural anisotropic surfaces. These results not only provide new insights into the anisotropic wetting phenomenon but also are beneficial to freely design anisotropic surfaces for bioinspired system application.

This work was supported by NSFC (Grant Nos. 60977025, 60525412, and 90923037).

- ¹L. Feng, S. H. Li, Y. S. Li, H. J. Li, L. J. Zhang, J. Zhai, Y. L. Song, B. Q. Liu, L. Jiang, and D. B. Zhu, *Adv. Mater.* **14**, 1857 (2002).
- ²Y. M. Zheng, X. F. Gao, and L. Jiang, *Soft Matter* **3**, 178 (2007).
- ³H. M. Whitney, M. Kolle, P. Andrew, L. Chittka, U. Steiner, and B. J. Glover, *Science* **323**, 130 (2009).
- ⁴Y. Y. Liu, X. Q. Chen, and J. H. Xin, *Bioinspir. Biomim.* **3**, 046007 (2008).
- ⁵P. Ball, *Nature (London)* **400**, 507 (1999).
- ⁶H. Gau, S. Herminghaus, P. Lenz, and R. Lipowsky, *Science* **283**, 46 (1999).
- ⁷B. Zhao, J. S. Moore, and D. J. Beebe, *Science* **291**, 1023 (2001).
- ⁸A. M. Higgins and R. A. L. Jones, *Nature (London)* **404**, 476 (2000).
- ⁹D. Y. Xia and S. R. J. Brueck, *Nano Lett.* **8**, 2819 (2008).
- ¹⁰M. Morita, T. Koga, H. Otsuka, and A. Takahara, *Langmuir* **21**, 911 (2005).
- ¹¹Y. Zhao, Q. H. Lu, M. Li, and X. Li, *Langmuir* **23**, 6212 (2007).
- ¹²A. D. Sommers and A. M. Jacobi, *J. Micromech. Microeng.* **16**, 1571 (2006).
- ¹³J. Y. Chung, J. P. Youngblood, and C. M. Stafford, *Soft Matter* **3**, 1163 (2007).
- ¹⁴D. Wu, Q. D. Chen, B. B. Xu, J. Jiao, Y. Xu, H. Xia, and H. B. Sun, *Appl. Phys. Lett.* **95**, 091902 (2009).
- ¹⁵H. B. Sun, A. Nakamura, S. Shoji, X. M. Duan, and S. Kawata, *Adv. Mater.* **15**, 2011 (2003).
- ¹⁶H. B. Sun, A. Nakamura, K. Kaneko, S. Shoji, and S. Kawata, *Opt. Lett.* **30**, 881 (2005).
- ¹⁷W. Li, G. P. Fang, Y. F. Li, and G. J. Qiao, *J. Phys. Chem. B* **112**, 7234 (2008).
- ¹⁸W. Li and A. Amirfazli, *J. Colloid Interface Sci.* **292**, 195 (2005).
- ¹⁹D. Wu, Q. D. Chen, H. Xia, J. Jiao, B. B. Xu, X. F. Lin, Y. Xu, and H. B. Sun, *Soft Matter* **6**, 263 (2010).
- ²⁰W. L. Min, B. Jiang, and P. Jiang, *Adv. Mater.* **20**, 3914 (2008).